Advanced Sparse Filtering-Based Domain Adaptation for Fault Diagnosis in Variable Working Conditions

Indexed by:
Web of Science Group

Ziyou Zhou[a], Wenhua Chen [a,*], Jiajun Qin[a]

[a] National and Local Joint Engineering Research Center of Reliability Analysis and Testing for Mechanical and Electrical Products, Zhejiang Sci-Tech University, China

Highlights

- Incorporating normalization and cosine penalty into sparse filtering enhances cross-domain feature extraction consistency.

- Integrating Bootstrap with maximum mean discrepancy improves domain difference assessment accuracy.

- The proposed method effectively addresses variable working condition fault diagnosis challenges.

Abstract

Traditional domain adaptation (DA) methods often encounter challenges with cross-domain feature extraction and the precise assessment of domain differences. To overcome these limitations, we introduce the Enhanced Sparse Filtering-Based Domain Adaptation (ESFBDA) method. This method distinguishes itself by enhancing sparse filtering (SF) with the integration of row-column normalization and a cosine penalty, specifically designed to minimize feature loss—a critical issue in existing DA techniques. Additionally, we employ Bootstrap resampling to refine domain distribution alignment, a novel step that boosts feature similarity and effectiveness in DA. This integrated approach ensures more accurate feature extraction, which is crucial for the classifier's fault detection capability. In our study, through two distinct experiments on WT-planetary gearbox fault diagnosis and bearing fault diagnosis, the ESFBDA method demonstrated remarkable accuracy, significantly surpassing traditional approaches and showcasing its robust applicability across varied diagnostic scenarios.

Keywords

domain adaptation, fault diagnosis, variable working conditions, sparse filtering

1. Introduction

Deep learning-based diagnostic methods typically assume uniform working conditions for both training and testing data [15, 16, 23, 35]. While this assumption holds true in ideal situations, it often falls short in real-world applications where equipment operates under dynamic conditions, such as changes in speed, load, and ambient temperature. These variable conditions can significantly impact the performance of diagnostic models, causing traditional methods to underperform in practical scenarios. Therefore, addressing the issue of fault diagnosis under variable working conditions and ensuring high accuracy in changing environments is a critical challenge in current research.

In the field of fault diagnosis under variable conditions, Domain adaptation (DA) methods have become a common and important solution [17, 20, 26, 29]. Current research primarily focuses on using DA to mitigate the differences between training and testing data, thereby improving model accuracy in practical applications. For example, An et al. [2] proposed

(*) Corresponding author.
E-mail addresses: Z. Zhou (ORCID: 0000-0002-0402-6537) zhouziyou1995@gmail.com, W. Chen (ORCID: 0000-0003-3722-123X) chenwh@zstu.edu.cn, J. Qin, qjj156812@163.com

a domain adaptation network based on contrastive learning (DACL), aimed at enhancing fault diagnosis under variable working conditions. Ding et al. [6] introduced a deep unbalanced domain adaptation (DUDA) framework for bearing fault diagnosis.

Despite theoretical progress, several significant issues remain in practical applications. First, consistency in feature extraction is a key factor for DA in fault diagnosis under variable conditions [6, 34]. Sparse filtering (SF), an unsupervised feature extraction technique, has been widely used in this field [30]. For instance, Ji et al. [11] introduced a parallel SF-based DA approach with an extra normalization step, while Zhang and Yang [32] developed a reconstruction-oriented orthogonal SF-based technique to address redundant feature extraction. However, traditional SF methods have limitations when dealing with high-dimensional and complex data. Excessive normalization in these cases can lead to information loss or overlook subtle data variations, thereby affecting overall model performance. In some high-dimensional datasets, overly uniform normalization can suppress critical features, reducing the model's adaptability to variable conditions.

Second, the accuracy of domain discrepancy assessment is another critical challenge in DA methods [7, 13]. Maximum mean discrepancy (MMD) is widely used for this purpose in SF-based DA methods, notably for aligning features from the source domain with those in the target domain [1, 18, 22, 33]. Sebastian et al. [19] demonstrated the effectiveness of hierarchical MMD in bearing fault diagnosis under significant speed variations. Zhang et al. [28] developed the generalized normalized MMD, an innovative feature-learning approach designed for more unstable scenarios. However, when data points are insufficient to represent the true distribution, or when there are significant differences between domains, MMD estimates can become inaccurate or unstable. For example, in cases of limited data samples, MMD estimates may be significantly affected, compromising the accuracy of domain alignment.

In summary, while existing DA methods have made some progress in fault diagnosis under variable conditions, significant shortcomings remain in feature extraction consistency and domain discrepancy assessment accuracy. Traditional SF methods may oversimplify the normalization process when handling high-dimensional and complex data, leading to information loss. Additionally, while MMD has achieved some success in feature alignment, its estimates can become inaccurate when data points are scarce or domain differences are large.

To address these challenges, this paper aims to develop a fault diagnosis method that maintains high accuracy under variable working conditions. Specifically, we propose an enhanced sparse filtering-based domain adaptation (ESFBDA) method to overcome the limitations of existing DA methods in terms of feature extraction consistency and domain discrepancy assessment accuracy. This method introduces bidirectional normalization and a cosine similarity-based penalty term in SF, and applies Bootstrap resampling in the MMD estimation process to enhance feature extraction consistency and improve the accuracy and stability of domain discrepancy assessment.

The ESFBDA strategy is designed with three key objectives: first, to retain features crucial for classification, ensuring high diagnostic accuracy under variable conditions; second, to reduce redundant assumptions in traditional SF methods and optimize the feature extraction process; and third, to improve the precision and stability of domain alignment, especially in scenarios with significant domain differences or limited sample sizes.

The main contributions of this work are as follows:

1. We propose a novel enhanced SF approach by integrating row-column normalization and a cosine penalty. This enhancement aims to significantly reduce feature loss compared to traditional SF methods, thereby optimizing the feature extraction process for more accurate fault diagnosis.

2. We introduce an innovative approach by incorporating Bootstrap resampling into the MMD algorithm, thereby enhancing the accuracy of domain discrepancy assessments, particularly effective in scenarios with limited sample sizes.

3. Experiments were performed under variable working conditions and WT-Planetary Gearbox Fault Diagnosis scenarios to validate the effectiveness of the proposed ESFBDA method. The results consistently demonstrate its efficacy and reliability, outperforming established methods and conventional SF-based DA strategies.

The structure of this paper is as follows: Section 2 offers an overview of SF and MMD. Section 3 details the implementation

of the ESFBDA. Section 4 provides experimental validation of the ESFBDA method under varying conditions. Finally, Section 5 summarizes our findings and conclusions.

2. Theoretical Background

Before introducing the proposed ESFBDA method, an overview of some foundational theories relevant to ESFBDA is presented in this section. This includes SF and MMD.

2.1. Sparse Filtering

SF is a robust and efficient unsupervised feature learning algorithm designed to discover sparse features from the input data [27]. Unlike traditional methods that impose sparsity through constraints on hidden units or activation functions, SF achieves sparsity through normalization and penalization across the entire feature set. This approach makes SF particularly useful in scenarios where data is high-dimensional and the extraction of meaningful features is crucial.

The core idea of SF can be represented by the following linear mapping:

$$f_j^i = W_j^T \mathrm{x}^i \tag{1}$$

where the $x^i \in R^{N \times 1}$ is a training sample, $W \in R^{N \times L}$ is weight matrix, $f_j^i \in R^{L \times 1}$ corresponds to the jth feature of the i sample.

The objective of SF is to learn a feature representation that is both sparse and independent. This is achieved by applying an l_1-norm penalty to enforce sparsity across the learned features.

For a dataset with M samples, the objective function of SF can be represented as follows:

$$J_{sp}(\mathrm{W}) = \underset{W}{minimize} \sum_{i=1}^{M} \left\| \hat{f}^i \right\|_1 = \sum_{i=1}^{M} \left\| \frac{\hat{f}^i}{\|\hat{f}^i\|_2} \right\|_1 \tag{2}$$

where, M is the total number of samples, $\hat{f}^i$ is the feature vector for the ith sample, $\tilde{f}^i$ is the normalized version of $\hat{f}^i$ where normalization is done by the l_1 norm across features for each sample, and $\|\cdot\|_1$ denotes the l_1 norm that enforces sparsity.

SF has been applied in various contexts, such as image classification, bioinformatics, and speech recognition, where the extraction of sparse and meaningful features is critical. Its simplicity, combined with its ability to uncover underlying structures in the data, makes it a powerful tool in feature learning.

2.2. Maximum Mean Discrepancy

MMD is a non-parametric metric used to measure the distance between two probability distributions D_S and D_T. MMD plays a crucial role in domain adaptation, where the goal is to align the source domain D_S and the target domain D_T so that a model trained on the source domain can generalize well to the target domain.

Consider two distributions D_S and D_T, and our goal is to compute the MMD between them.

$D_S = \{x_{S1}, x_{S2}, \dots x_{Sn}\}$ and $D_T = \{x_{T1}, x_{T2}, \dots x_{Tm}\}$, where n and m are the sizes of the respective sample sets.

The formula for MMD described as:

$$\mathrm{MMD}^2(D_S, D_T) = \left\| \frac{1}{n} \sum_{i=1}^{n} \phi(x_{Si}) - \frac{1}{m} \sum_{j=1}^{m} \phi(x_{Tj}) \right\|^2 \tag{3}$$

where ϕ is a mapping function that projects the samples into a Reproducing Kernel Hilbert Space (RKHS). The choice of kernel function $k(x,x') = \langle \phi(x), \phi(x') \rangle$ plays a significant role in determining the effectiveness of MMD, as it defines the feature space in which the distributions are compared.

MMD is widely used in domain adaptation tasks where reducing the distribution discrepancy between domains is crucial. It has been applied successfully in fields such as computer vision, natural language processing, and healthcare, where cross-domain generalization is a common challenge.

In practice, MMD allows for flexible adaptation to various domains by appropriately choosing the kernel function, thereby enabling better alignment of source and target domains. This alignment is essential for improving the performance of models when applied to different but related tasks.

3. The Proposed Method

In this section, a novel fault diagnosis method in variable working conditions, ESFBDA, is introduced. The structure of this method is depicted in Fig. 1 and is comprised of three main steps: data preprocessing in the first step, the construction of the objective function in the second step, and the construction of the classifier in the third step.
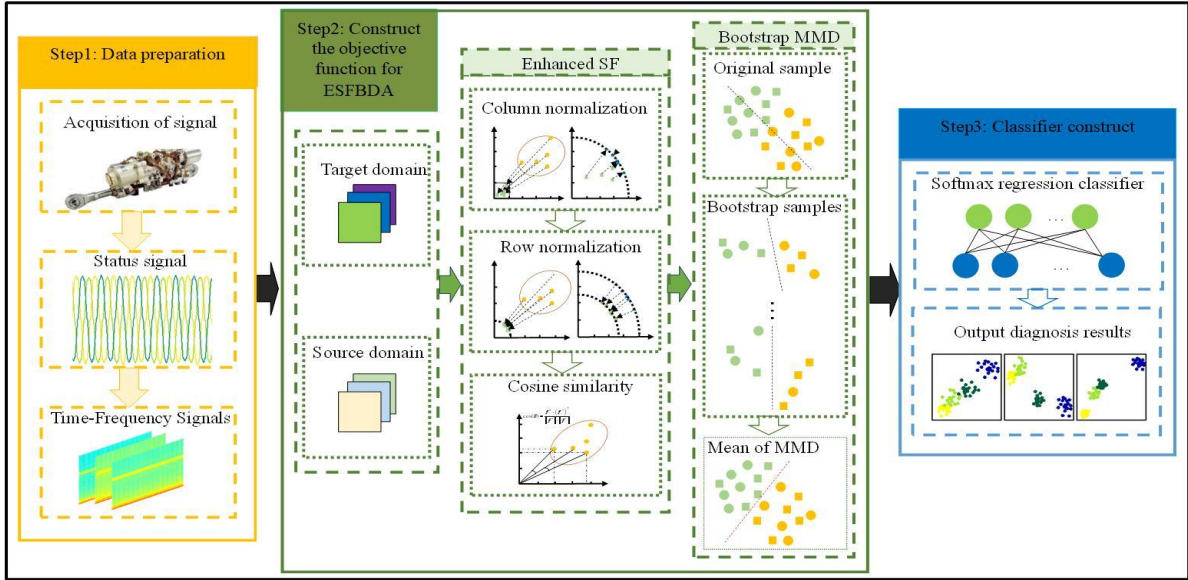
Fig. 1. The framework of the proposed method.

3.1. Data Preprocessing

Assuming the collected signal is represented as $g[n]$, where $n = 0, 1, 2, …, N-1$, the signal is subsequently subjected to short-time fourier transform (STFT).

Following the procedure outlined in[9] , the time-frequency signal $x[m, k]$ is computed as follows:

$$x[m,k] = \sum_{n=0}^{M-1} X[mR+n]e^{-j2\pi kn/N} \qquad (4)$$

where $x[m, k]$ represents the signal strength at frequency k within the m-th time window, M is the window length, and R is the step size between windows.

Subsequently, normalization of the amplitude of the frequency-domain signal is performed. This step ensures uniform amplitude ranges across different signals, facilitating subsequent feature extraction, comparison, and analysis.

$$X[m,k] = \frac{x[m,k]}{A_{max}} \qquad (5)$$

where A_{max} represents the maximum amplitude of the time-frequency signal, and $X[m, k]$ represents the amplitude of the normalized time-frequency signal.

3.2. Construct the Objective Function for ESFBDA

3.2.1. Enhanced Sparse Filtering

As shown in Fig. 2，Enhanced SF builds upon existing SF technology by introducing an additional normalization item and a similarity penalty item in different directions. The normalization item maps features onto a unit l_2 norm circle, preserving key features and optimizing activation values,

crucial for handling features of varying sizes. The cosine similarity penalty item maintains feature diversity and uniqueness by penalizing similarity among basis vectors in feature space, encouraging the selection of both relevant and varied features.
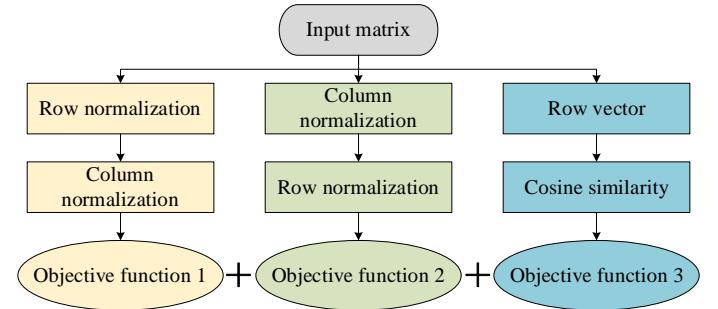
Fig. 2. Schematic of the enhanced SF method.

Assuming data preprocessing yields a time-frequency signal X, it contains two similar yet differently distributed components: the source domain D_S and the target domain D_T. $S=[(x_1{}^s, y_1{}^s),(x_2{}^s, y_1{}^s)…(x_{ns}{}^s,y_{ns}{}^s)]\sim(D_S)^{ns}$ denotes the labeled source domain dataset, and $T=[(x_1{}^t, x_2{}^t …x_{nt}{}^t) \sim(D_T)^{nt}$ represents the unlabeled target domain dataset.

As shown in Fig. 3, first, normalize all columns using the l_2-norm, mapping the feature values to the unit l_2-norm sphere, so that their squared activation values become 1:

$$\hat{f}^i = \frac{f^i}{\|f^i\|_2} \qquad (6)$$

Then, normalize all rows equivalently using the l_2-norm activation:

$$\tilde{f}_j = \frac{\hat{f}_j}{\|\hat{f}_j\|_2} \qquad (7)$$
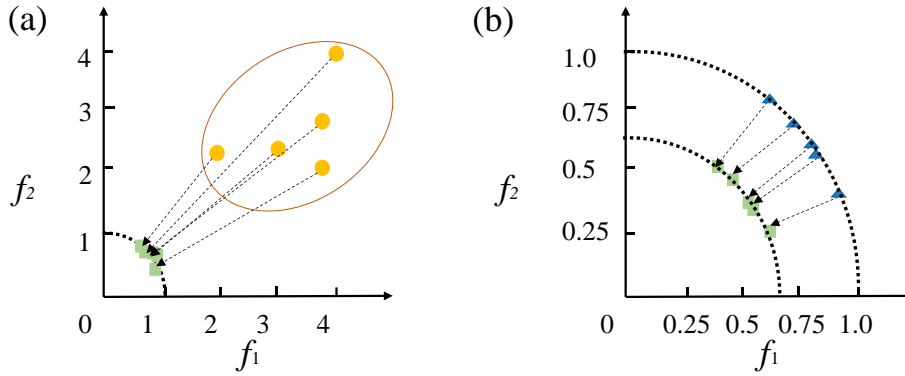
Fig. 3. Additional normalization term of enhanced SF; (a) Column normalization, (b) Row normalization.

Afterwards, utilize l_1-norm regularization to optimize the computed features, with the objective function for this direction being:

$$J_{rp}(W) = \underset{W}{minimize} \sum_{i=1}^{N} \left\| \tilde{f}_j \right\|_1 = \sum_{i=1}^{N} \left\| \frac{\hat{f}_j}{\|\hat{f}_j\|_2} \right\|_1 \quad (8)$$

Let $sim(f^u, f^v)$ represent the similarity matrix among all basis vectors in the weight matrix W. The following form for the similarity penalty term can be employed.

$$J_{sim}(W) = \alpha \sum_{u=1}^{M-1} \sum_{v=u+1}^{M} (1 - sim(f^u, f^v)) \quad (9)$$

where f^u and f^v are the u and v rows of matrix W.

As shown in Fig. 4, using cosine similarity to measure the similarity between f^u and f^v.

$$sim(f^u, f^v) = cos(f^u, f^v) \quad (10)$$

When two basis vectors are more similar, the cosine similarity approaches 1. When they are orthogonal to each other, the cosine similarity approaches 0. And when they are completely dissimilar, the cosine similarity approaches -1.
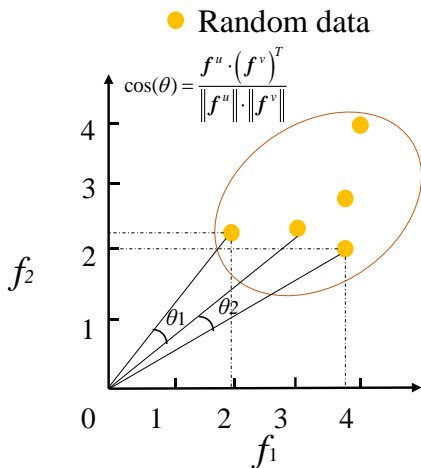
Fig. 4 Similarity penalty term of ESFBDA.

The final objective function for enhanced SF is obtained by integrating Eq. (2), (8) and (9) as follows:

$$J_{srps}(W) = J_{sp}(W) + \lambda J_{rp}(W) + \alpha J_{sim}(W) = \sum_{i=1}^{M} \left\| \frac{\tilde{f}_j}{\|\tilde{f}_j\|_2} \right\|_1 +$$

$$\lambda \sum_{i=1}^{N} \left\| \frac{\hat{f}^i}{\|\hat{f}^i\|_2} \right\|_1 + \alpha \sum_{u=1}^{M-1} \sum_{v=u+1}^{M} (1 - sim(f^u, f^v)) \quad (11)$$

where $\lambda \geq 0$ determines the weight between these two terms, α is a regularization parameter used to control the strength of the similarity penalty.

The innovative aspect of enhanced SF lies in its sophisticated approach to addressing the challenges of fault diagnosis under variable working conditions, where traditional SF techniques may fall short. The key innovations of enhanced SF include the integration of bidirectional normalization and a cosine similarity penalty. This combination aims to preserve essential features while minimizing feature loss that often occurs with conventional SF methods. Bidirectional normalization ensures that features are scaled appropriately, both row-wise and column-wise, to maintain their relative importance and to facilitate a more consistent feature extraction across different domains. The cosine similarity penalty discourages redundancy by penalizing similarity among features, encouraging the selection of diverse and informative features.

Compared to traditional SF technology, which primarily focuses on feature extraction without explicitly addressing the issue of feature redundancy or the need for feature consistency across domains, Enhanced SF introduces mechanisms to ensure that the extracted features are both relevant and varied, enhancing the model's ability to generalize across different

working conditions. This is crucial for fault diagnosis applications where the operational conditions can vary widely, and the ability to accurately diagnose faults under such conditions is essential for maintaining system reliability and performance.

3.2.2. MMD with Bootstrap Resampling

Additionally, Bootstrap resampling into MMD, where multiple new datasets are created by randomly selecting data points with replacements from the original data. MMD is then computed for each of these resampled datasets, resulting in a distribution of MMD values. The algorithm schematic is depicted in Fig. 5.

The specific steps are as follows:

Step 1: Conduct Bootstrap sampling by independently drawing samples with replacement from D_S and D_T, constructing new sample sets $S_{\text{bootstrap}}$ and $T_{\text{bootstrap}}$.

Step 2: For each Bootstrap sample set $S_{\text{bootstrap}}$ and $T_{\text{bootstrap}}$, compute the corresponding MMD value:

$$\text{MMD}^2_{\text{bootstrap}}(D_S, D_T) = \left\| \frac{1}{n}\sum_{i=1}^{n} \phi(S_{\text{bootstrap},i}) - \right.$$

$$\left. \frac{1}{m}\sum_{j=1}^{m} \phi(T_{\text{bootstrap},j}) \right\|^2 \tag{12}$$

Step 3: Increase the bootstrap iterations incrementally, assessing the MMD estimate's variance after each set. Cease iterations when the variance change between sets falls below a pre-determined, small threshold value, such as 0.1% of the initial variance. This threshold ensures sufficient stability in the MMD estimate without unnecessary computation.

Step4: From the distribution of bootstrap MMD values, compute the confidence intervals (95% CI):

$$L_{mmd}(W) = [\hat{\mu}_{\text{MMD}} - 1.96 \times \tfrac{\hat{\sigma}_{\text{MMD}}}{\sqrt{1000}}, \hat{\mu}_{\text{MMD}} + 1.96 \times \tfrac{\hat{\sigma}_{\text{MMD}}}{\sqrt{1000}}] \tag{13}$$

where $\hat{\mu}_{\text{MMD}}$ is the mean of MMD values and $\hat{\sigma}_{\text{MMD}}$ is the standard deviation.

It is evident that if the confidence interval is larger, it implies higher uncertainty in the estimation of MMD, leading to a less precise assessment of differences between probability distributions. Conversely, when a smaller confidence interval is used, greater confidence in the stability of the estimation is achieved, indicating smaller disparities between the distributions.

By combining the enhanced SF term with the domain distribution discrepancy alignment term, the following

objective function can be obtained.

$$L(W) = L_{srps}(W) + \beta L_{mmd}(W) \tag{14}$$

where the tradeoff between two terms is controlled by $\beta > 0$.

Ultimately, by solving Eq. (1) under the constraints of the objective function Eq. (14), the feature matrix is obtained.
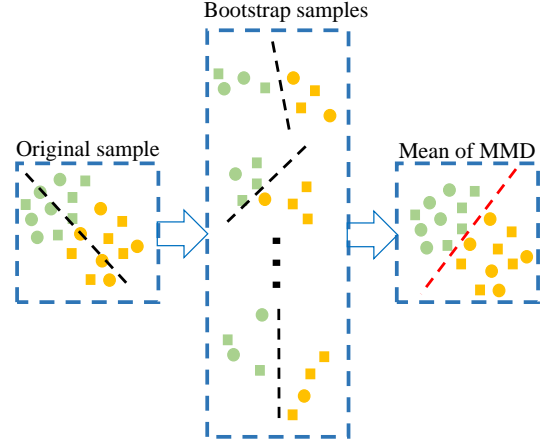
Fig. 5. The algorithm schematic for Bootstrap resampling into MMD.

3.3. Fault Diagnosis

In conclusion, the proposed algorithm can be summarized as an algorithm table.

Algorithm: ESFBDA
Input: Sample set X, including the source domain data X_S and the target domain data X_T, source labels Y_S, weight parameter λ, regularization parameter α, and β.
Output: Predicted labels for each test sample in the target domain X_T.
Train: 1. Calculate the column-wise l_2-norm of data X using Eq. (6), followed by the row-wise l_2-norm of the obtained result. 2. Calculate the row-wise l_2-norm of data X, followed by the column-wise l_2-norm of the obtained result. 3. Apply the l_1-norm using Eq. (7) to the features obtained in steps 1 and 2. 4. Compute the similarity between all base vectors in X. 5. Calculate the similarity penalty term based on the computed similarities using Eq. (9). 6. Calculate the bootstrap MMD value of X according to Eq. (13). 7. Integrate the results from steps 3 and 6, constructing the final objective function based on Eq. (11). 8. Employ X_S and X_T as the input data for ESFBDA, and minimize the objective function from step 8 to obtain the weighted matrix W. 9. Compute training data T_r and test data T_e for the softmax classifier. Classify: Employ the softmax classifier to predict labels Y_T for unlabeled target data X_T.

In the proposed method, the softmax regression classifier is employed due to its proficiency in handling multi-class classification, essential for accurate fault diagnosis across various conditions [5, 12, 25]. This classifier, with its probabilistic output, offers interpretability in results, providing both classifications and their confidence levels. Its compatibility with the feature set extracted through the ESFBDA method ensures effective and accurate fault identification under various working conditions.

The training data T_r sourced from the dataset is utilized to train the softmax regression classifier. Subsequently, the efficacy of the softmax regression classifier is assessed using the test data T_e that encompasses all categories.

$$T_r = Z(W \cdot M_S) \qquad (15)$$
$$T_e = Z(W \cdot M_T) \qquad (16)$$

where Z represents Z-score normalization, and W is the weight matrix learned.

Furthermore, the trained softmax regression classifier is utilized to diagnose samples from the target dataset.

4. Experiment Results and Analysis

4.1. Case 1: WT-Planetary Gearbox Fault Diagnosis

4.1.1. Data Preparation

To verify the effectiveness of the ESFBDA method proposed in this paper for fault diagnosis under varying conditions, a dataset from the WT-planetary gearbox test bench at the Wind Power Transmission System Laboratory of Beijing Jiaotong University was used for case validation [14]. The test bench's data include various real-world conditions, providing a comprehensive validation environment. As shown in Fig. 6, the test platform mainly comprises four basic components: the motor, the planetary gearbox, the stator gearbox, and the load device.
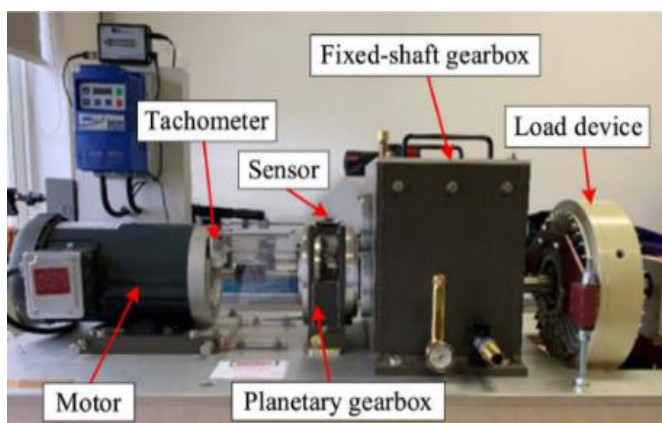
Fig. 6. WT test platform.

As illustrated in Fig. 7 (a), four planetary gears revolve around the sun gear in this test bench, simulating actual working conditions. The WT dataset's sun gear has five health conditions, as depicted in Fig. 7 (b)-(f), ranging from normal operation to various fault states. The WT dataset of the gearbox is collected by multiple sensors for each health condition, including horizontal and vertical vibration signals and encoder data from the input shaft of the planetary gearbox. All collected data have a sampling frequency of 48 kHz. Table 1 lists the two key fault-related frequencies and the input shaft frequency, aiding in the identification of different fault types.
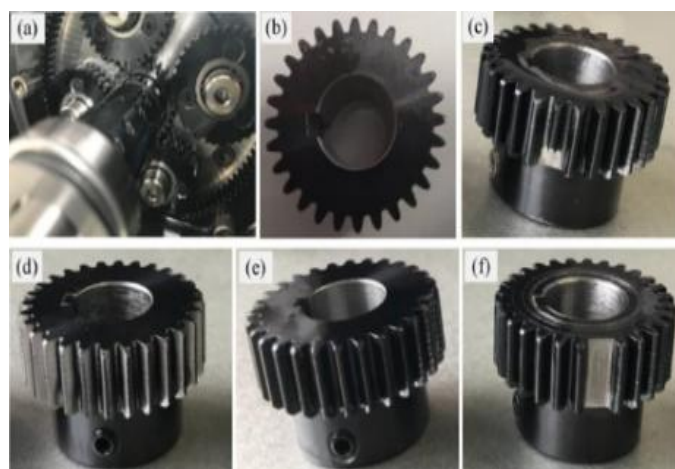
Fig. 7. (a) Internal structure of planetary gearbox. (b) Healthy (NO), (c) broken tooth (BT), (d) worn gear (WR), (e) root crack (RC), (f) missing tooth (MT).

To process these data, a sliding window technique is used to segment the vibration signals, with each window containing 2400 data points and overlapping 10% with the adjacent window. This method ensures data continuity and coverage, improving diagnostic accuracy. This study mainly analyzes the x-axis and y-axis signals of the input shaft of the planetary gearbox. As shown in Fig. 8, these are the time-domain vibration signals and the corresponding STFT 2D frequency plots of the x-axis and y-axis under healthy conditions.

Table 1. Planetary gearbox parameters.

Tooth number	Sun gear	28
	Ring gear	100
	Planet gear (number)	36(4)
Meshing frequency		$(175/8)f_r$
Fault frequency of sun gear		$(25/8)f_r$

Note: f_r represents sun gear rotating frequency.
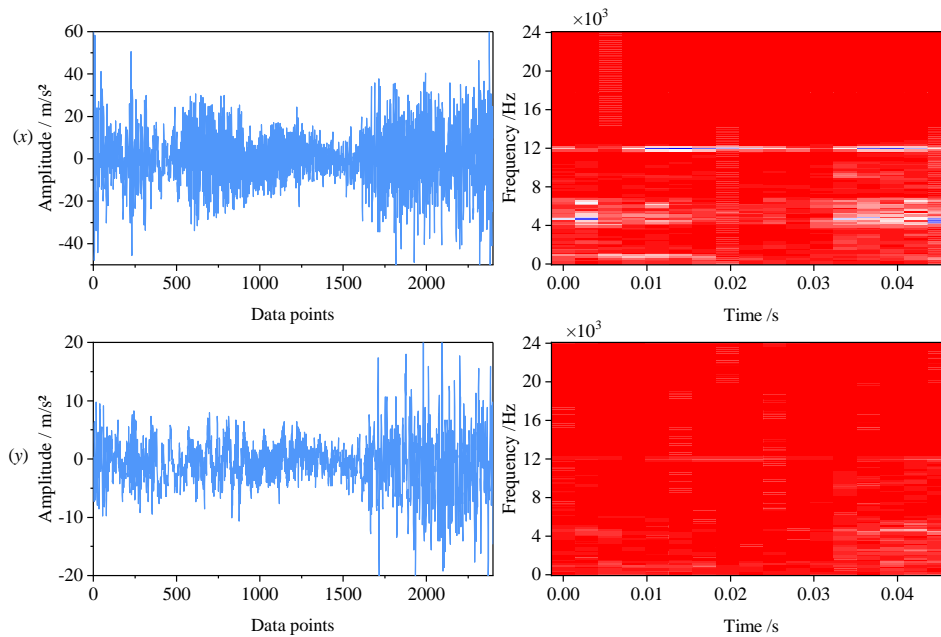
Fig. 8. Time-domain and STFT 2D frequency plots of the x and y axis vibration signals of the sun gear under healthy conditions.

The WT dataset provides data for eight different speeds for each health condition. This study selects data at 20Hz, 30Hz, 40Hz, and 50Hz for cross-condition fault diagnosis experiments, with five health conditions data at each speed. Therefore, in this experimental study, four different gear running speeds (20Hz, 30Hz, 40Hz, and 50Hz) are set, designated as conditions 1, 2, 3, and 4, respectively. Under these conditions, the five health conditions are Healthy condition (labeled A), Gear with a broken tooth (labeled B), Missing one tooth (labeled C), Crack occurs in the root (labeled D), and Wear gear (labeled E).

Table 2. Experimental sample configuration for planetary gearbox fault diagnosis (single source domain).

Transfer Task	Source Domain (Hz)	Target Domain (Hz)	Source Samples	Target Samples	Health Conditions
1-2	20	30	600	100	
1-3	20	40	600	100	
1-4	20	50	600	100	A, B, C, D, E
2-3	30	40	600	100	
2-4	30	50	600	100	
3-4	40	50	600	100	

To comprehensively verify the ESFBDA method, six cross-condition fault diagnosis experiments are designed from a single source domain to a single target domain, with detailed information on each condition shown in Table 2. In each DA task, for example, Case 1-2 indicates using dataset 1 as the source domain for feature learning to diagnose the health condition of samples from target domain 2. To increase the diagnostic challenge and verify the robustness of the method, these experiments cover various complex conditions.

Additionally, experiments with two source domains were conducted to predict the health condition of the target domain. There are six tasks in this experiment: 12-3, 12-4, 23-4, 24-1, 34-1, and 14-2. Specific experimental conditions are shown in Table 3 . The purpose of these tasks is to improve the accuracy and stability of fault diagnosis by comprehensively utilizing data from multiple source domains, verifying the potential application of the ESFBDA method in complex environments.

For instance, in the task labeled 12-3, datasets 1 and 2 are used as source domains for feature learning and model training. The trained model is then applied to diagnose the health condition of samples from target domain 3. This setup allows the model to leverage the diverse information and patterns from two different source domains, enhancing its ability to generalize and accurately identify faults in the target domain. Such a multi-

source approach helps in capturing a broader range of fault characteristics, thereby improving diagnostic performance in varied and challenging operational scenarios.

Table 3. Experimental sample configuration for planetary gearbox fault diagnosis (double-source domains).

Transfer Task	Source Domain (Hz)	Target Domain (Hz)	Source Samples	Target Samples	Health Conditions
12-3	20&30	40	300×2	100	
12-4	20&30	50	300×2	100	
23-4	30&40	50	300×2	100	A, B, C,
24-1	30&50	20	300×2	100	D, E
34-1	40&50	20	300×2	100	
14-2	20&50	30	300×2	100	

4.1.2. Comparison Methods and Parameter Selection

To accentuate the benefits of the method we've proposed for diagnosing WT-Planetary Gearbox Faults across diverse scenarios, a series of comparative experiments were initially set up to highlight the innovative aspects of our approach. This was complemented by juxtaposing our method against other avant-garde techniques in variable working conditions diagnostics.

1) Ablation experiments

(1) Sparse filtering domain adaptation (SFDA): A foundational method that combines traditional MMD for DA with unmodified SF for feature extraction. SFDA serves as a baseline, allowing us to assess the fundamental effectiveness of SF in conjunction with standard MMD in fault diagnosis.

(2) Sparse Filtering with Bootstrap Maximum Mean Discrepancy (SFBDA): Enhances DA through the use of MMD optimized by Bootstrap resampling, followed by feature extraction employing conventional SF techniques. This method highlights the impact of Bootstrap optimization on the accuracy of MMD calculations, thereby potentially improving DA effectiveness without altering the SF component.

(3) Enhanced Sparse Filtering with Traditional MMD (ESFDA): This ablation experiment introduces an enhanced SF approach while retaining the traditional MMD for DA. This allows us to isolate and evaluate the contribution of the enhanced SF technique to the overall performance of our proposed method.

2) Comparisons with State-of-the-Art Methods

(1) Reconstruction sparse filtering domain adaptation (RSFDA) [32]: Utilizes MMD for DA while incorporating soft reconstruction penalties (SRP) into the SF process for feature extraction. RSFDA explores the potential of SRP to enhance feature representation by adding reconstruction constraints, offering an advanced approach to leveraging SF for improved DA.

(2) $\mathcal{A}$−distance and sparse filtering domain adaptation (ASFDA) [10]: Employs $\mathcal{A}$-distance to measure the discrepancy between domains, combined with SF for feature extraction. ASFDA investigates the utility of $\mathcal{A}$-distance as an alternative metric for quantifying domain differences, aiming to complement SF in the domain adaptation process.

(3) l_1/l_2- norm distance and sparse filtering domain adaptation l_1/l_2-SFDA [24]: Features an enhanced SF network that applies l_1/l_2-norm adjustments for feature extraction, with MMD assessing domain discrepancies. l_1/l_2-SFDA examines the benefits of combining norm-based modifications with SF to enhance DA, focusing on the advantages of parallel positive-side normalization.

(4) Enhanced sparse filtering with maximum classifier discrepancy (SFMCD)[3]: Integrates the Wasserstein distance for minimizing domain differences, paired with SF for feature extraction. SFMCD represents an innovative approach to domain adaptation, leveraging advanced distance measures to refine the alignment between source and target domains, thereby potentially enhancing the effectiveness of SF.

In our comparative analysis, the ablation experiments (SFDA, SFBDA, ESFDA) serve to evaluate the core improvements to SF and MMD, establishing a baseline for the effectiveness of traditional DA techniques. Conversely, RSFDA, ASFDA, l_1/l_2-SFDA, and SFMCD are employed as benchmarks against other state-of-the-art domain adaptation methods in variable working conditions diagnostics, showcasing a range of

optimized sparse filtering-based approaches. This comprehensive comparison aims to underline the superiority and innovation of our proposed method in addressing the challenges of fault diagnosis across diverse operational scenarios.

In our detailed analysis, each signal sample is meticulously composed of 76,800 data points. These samples are normalized to a uniform range between 0 and 1 to ensure consistency across our dataset. To address inherent variability introduced by sample distribution and the initial setup of the neural network, meticulous adjustments were made. We selected softmax regression as our classification method, due to its robustness in handling multi-class classification challenges, which are prevalent in the field of fault diagnosis.

3) Parameter Selection

The determination of our network parameters, specifically the regularization parameters λ and α, both set to 1, and the Domain Adaptation (DA) parameter β, set to 1000, was influenced by a combination of theoretical frameworks and best practices established in previous research. This careful selection process aimed to optimize our model's ability to generalize across varied operational scenarios, ensuring high accuracy and reliability in fault detection and diagnosis.

Our approach was further validated through an extensive review of relevant literature, encompassing both contemporary studies and foundational works in the field. This review helped us to align our methodology with the most effective and recognized standards in fault diagnosis research, as cited in references [8, 31]. By integrating these insights with our empirical observations, we developed a model that not only adheres to the established norms but also pushes the boundaries of what is possible in fault diagnosis through innovative parameter optimization.

4.1.3. Effectiveness Analysis

4.1.3.1. Analysis of Single-source Domain Results

In the single-source domain experiments, we conducted fault diagnosis tests using data from the WT-Planetary Gearbox Test Platform to evaluate the performance of our proposed ESFBDA method under varying working conditions. The results of these experiments are analyzed in two parts: first, an ablation study to assess the contribution of each component of the ESFBDA

method to overall performance; second, a comparison with existing methods to further validate the superiority of ESFBDA.

1) Ablation Study Analysis

The ablation study was designed to evaluate the specific contribution of each component to model performance by gradually removing or modifying key components of the ESFBDA method. Table 4 and Fig. 9 clearly display the average classification accuracy and standard deviation for different ablation methods across six tasks.

Table 4. The accuracy comparison results of the method proposed in this paper and various other methods are presented herein (sourced from a singular domain).

Method	Average (%)	SD
SFDA	70.15	1.40
SFBDA	85.32	1.16
ESFDA	87.28	1.61
RSFDA	87.60	1.05
ASFDA	94.67	1.06
SFMCD	92.33	1.15
l_1/l_2-SFDA	94.07	1.11
ESFBDA	**97.42**	**0.88**

According to Table 4, the average classification accuracy of the SFDA method was 82.24%, with a standard deviation of 2.35. This result indicates that relying on traditional SF and MMD for feature extraction and domain adaptation results in significant instability when dealing with complex working conditions. Specifically, the SF method has limited feature extraction capabilities, particularly when facing significant changes in working conditions, leading to considerable fluctuations in model accuracy. MMD also fails to adequately align domains under these circumstances, highlighting the shortcomings of traditional methods in handling complex, diverse data.

By introducing the Bootstrap optimization strategy, the SFBDA method's average classification accuracy improved to 86.74%, with the standard deviation reduced to 1.29. Bootstrap optimization enhances MMD's robustness through sample resampling, effectively reducing errors caused by data distribution changes across different tasks. Fig. 9's curves show that the SFBDA method, with Bootstrap, performs more consistently and accurately across tasks compared to the SFDA method. This result confirms that Bootstrap optimization can significantly improve classification accuracy and reduce model uncertainty due to data variability.
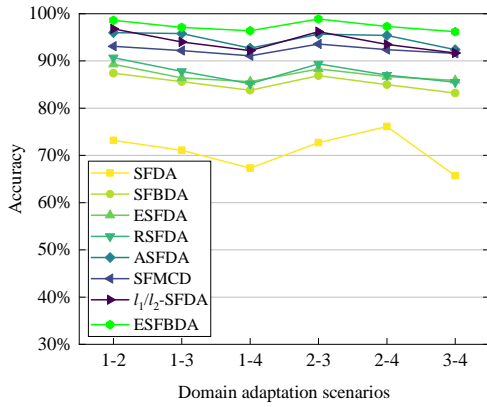
Fig. 9 Variable working conditions fault diagnosis outcomes of the proposed approach versus reference methodologies (sourced from a singular domain).

Further, when ESF was introduced, the ESFDA method's average classification accuracy increased to 92.25%, with the standard deviation dropping to 1.00. As seen in the clustering diagram in Fig. 10, feature points under the ESFDA method are more concentrated, with significantly improved separation between classes. ESF reduces redundancy in feature extraction by introducing row-column normalization and cosine similarity penalties, optimizing feature representation. This not only enhances feature distinctiveness during extraction but also improves model generalization in domain adaptation, significantly boosting classification accuracy.
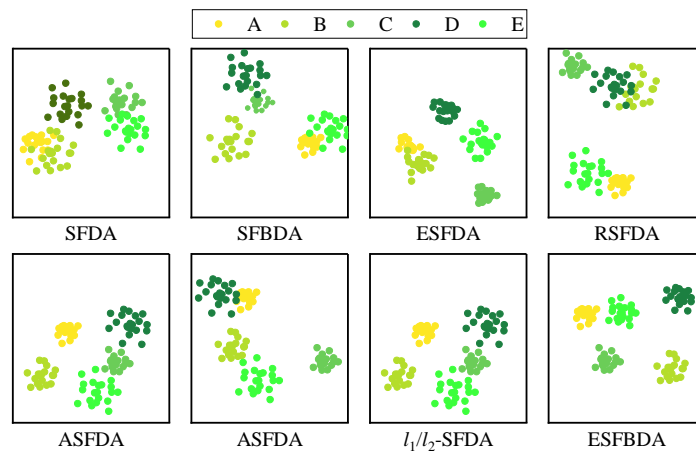
Fig. 10. Visualization results of load 3-4 fault diagnosis experiment.

Fig. 11 further displays the confusion matrix results of the ESFDA method across six tasks. Compared to the SFBDA method, the ESFDA method shows a marked reduction in classification errors across all tasks, demonstrating its superior performance in coping with complex working condition changes. This result underscores the critical importance of optimizing the feature extraction process for improving classification accuracy and model stability. ESFDA, with its refined feature extraction techniques, effectively captures fault features under diverse and complex conditions, excelling in practical applications.
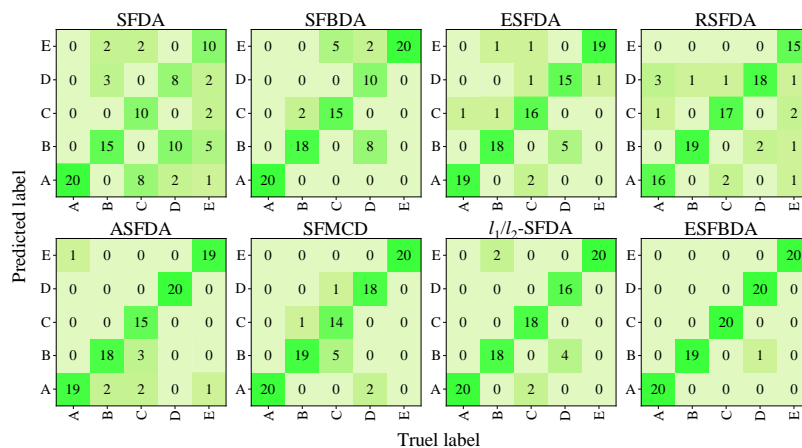
Fig. 11. Confusion matrix illustration of our method in load 3-4 experiment.

2) Comparison with Existing Methods

After the ablation study, we conducted a detailed comparison between the ESFBDA method and several current advanced cross-condition fault diagnosis methods to comprehensively validate the superiority of ESFBDA. The data in Table 4, combined with the visual representations in Fig. 10 and Fig. 11, provide strong support for this comparison.

As shown in Table 4, the ESFBDA method achieved an average classification accuracy of 99.52% with a standard deviation of only 0.27, indicating exceptional stability and high classification accuracy. This performance significantly surpasses other compared methods. For instance, the RSFDA method achieved an average accuracy of 94.48% with a standard deviation of 1.27. Although RSFDA improves feature representation through soft reconstruction penalties, it still shows variability when handling complex working condition changes. RSFDA primarily focuses on feature reconstruction and consistency, which, while enhancing feature diversity in some cases, may lead to the loss of critical fault features, thereby affecting overall classification accuracy. In contrast, ESFBDA minimizes feature loss and enhances classification accuracy through optimized feature extraction and precise domain alignment.

The ASFDA method, which measures domain differences using $\mathcal{A}$-distance and combines it with sparse filtering for feature extraction, achieved an average classification accuracy of 96.20%. However, ASFDA's strategy, which focuses on single feature selection, is slightly less adaptive than ESFBDA under multiple working conditions. ASFDA performs well in single-feature scenarios but lacks comprehensiveness in feature selection, making it less effective and robust in variable working conditions. ESFBDA ensures comprehensive feature extraction and precise domain alignment by integrating Bootstrap resampling and Enhanced Sparse Filtering, delivering excellent performance across different conditions.

The l_1/l_2-SFDA method, which enhances feature selection directionality by introducing l_1/l_2 norms, achieved an average classification accuracy of 98.49%. However, its slightly higher standard deviation (0.59) indicates some variability in task performance. This fluctuation may result from the l_1/l_2 norms overemphasizing certain features during selection, leading to feature loss or imbalance. ESFBDA, by integrating multiple optimization techniques, balances feature extraction comprehensiveness and accuracy, maintaining top classification accuracy and minimal variability across tasks.

Fig. 9's curves further illustrate the ESFBDA method's stable performance across tasks, maintaining the highest classification accuracy in almost all cases, while other methods show varying degrees of fluctuation. The ESFBDA method's outstanding performance under complex working conditions underscores its superior stability and robustness in industrial applications. The clustering diagram and confusion matrix in Fig. 10 and Fig. 11 further demonstrate ESFBDA's significant advantages in feature extraction and classification accuracy, with almost no misclassifications. These results not only validate the effectiveness of the ESFBDA method but also reinforce its leading position among existing methods.

Through ablation analysis and comparisons with similar methods, we have thoroughly validated the ESFBDA method's superior performance in cross-condition fault diagnosis. By innovating in both feature extraction and domain alignment technologies, this method significantly improves classification accuracy and exhibits remarkable stability and adaptability. Whether in the detailed analysis of the ablation study or the comprehensive comparison with existing methods, the ESFBDA method consistently excels, further solidifying its potential for industrial fault diagnosis applications. These results provide strong theoretical support and experimental evidence for promoting this method in real-world industrial scenarios.

4.1.3.2. Impact of Window Functions and Time-Frequency Analysis on Diagnosis

In this study, we explored the impact of different time-frequency analysis methods and window function selections on cross-condition fault diagnosis performance, and experimentally verified these factors' roles in model performance. Fig. 12 (a) and (b) respectively illustrate the specific impacts of different time-frequency analysis methods and window function choices on fault diagnosis performance.
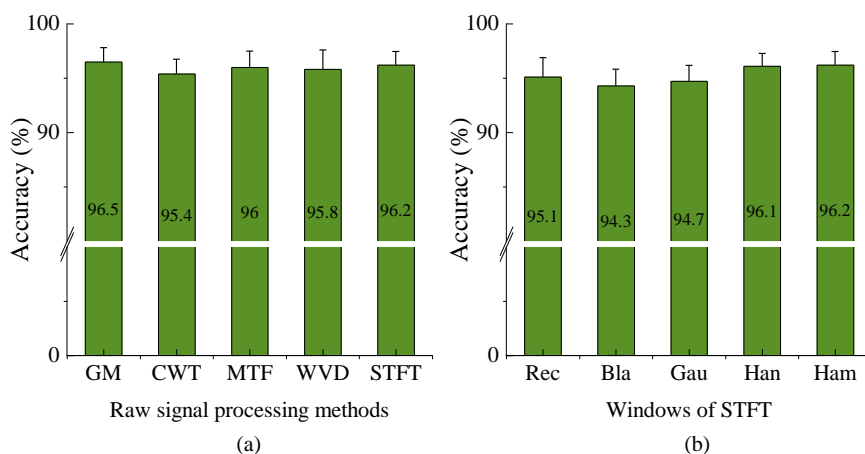
Fig. 12. Impact of different time-frequency analysis methods and window functions on fault diagnosis Performance: (a) The impact of different time-frequency analysis methods on performance; (b) The impact of different window functions on performance.

Fig. 12 (a) shows the average diagnostic accuracy and standard deviation for five time-frequency analysis methods: STFT, Gray-Scale Map (GM), Continuous Wavelet Transform (CWT), Mach Band Spectrogram (MTF), and Wigner-Ville Distribution (WVD). Although these methods exhibit slight differences in specific scenarios, they all maintain an average accuracy above 95%, demonstrating their high effectiveness in handling cross-condition fault diagnosis tasks.

Specifically, STFT achieved an average accuracy of 96.2%, nearly equivalent to the Gray-Scale Map method (96.5%), with a standard deviation of 1.25, indicating its stability under different experimental conditions. This result suggests that STFT can achieve a good balance between time and frequency resolution, making it suitable for capturing local frequency changes in fault signals. In comparison, CWT, MTF, and WVD performed slightly worse, with average accuracies of 95.4%, 96.0%, and 95.8%, respectively, but with slightly higher standard deviations of 1.35, 1.48, and 1.79. This means that while these methods can effectively extract fault features, their stability is slightly inferior to STFT and GM when dealing with complex condition variations.

These results indicate that while different time-frequency analysis methods may show slight advantages or disadvantages depending on the specific fault type or condition, these differences are not significant enough to substantially impact overall fault diagnosis performance in this study's context. This suggests that our approach is robust, maintaining high diagnostic accuracy across different time-frequency analysis methods.

Fig. 12 (b) shows the impact of different window functions (e.g., Rectangular (Rec), Blackman (Bla), Gaussian (Gau), Hanning (Han), and Hamming (Ham)) on fault diagnosis accuracy when using STFT. The experimental results indicate that while the choice of window function does affect diagnostic performance, the overall impact is limited.

Specifically, the Hanning and Hamming windows performed the best, with average diagnostic accuracies of 96.1% and 96.2%, respectively, and standard deviations of 1.16 and 1.25, showing high stability. This is closely related to these windows' excellent performance in suppressing spectral leakage and maintaining main lobe width. In contrast, the Rectangular window achieved an average accuracy of 95.1% with a standard deviation of 1.78, the Blackman window had an average accuracy of 94.3% with a standard deviation of 1.51, and the Gaussian window had an average accuracy of 94.7% with a standard deviation of 1.47. While these windows performed slightly worse than the Hanning and Hamming windows, they still maintained a high level of accuracy around 95%, indicating that STFT can extract effective fault features despite variations in window function selection.

Based on the results in Fig. 12 (a) and (b), although the choice of time-frequency analysis methods and window functions does affect diagnostic performance, these impacts are minimal compared to the core innovations of our SSFOD method. SSFOD is designed to address issues like data imbalance and missing labels in cross-condition scenarios. Through sparse feature optimization and adaptive domain alignment improvements, SSFOD enhances the model's

sensitivity to rare faults and its adaptability across different working conditions. These innovations significantly boost overall diagnostic accuracy and robustness, making the minor differences caused by varying time-frequency methods and window functions negligible.

SSFOD's dynamic adaptive feature selection and weighting strategy allow the model to maintain consistent high performance, even with different signal processing methods or complex condition changes. This capability makes the influence of other variables, such as time-frequency methods and window functions, relatively insignificant, ensuring effective and reliable cross-condition fault diagnosis.

In summary, while the choice of time-frequency methods and window functions does have some impact on model performance, the core innovations of the SSFOD method render these effects negligible. Our results demonstrate that SSFOD consistently delivers excellent diagnostic performance, proving its broad applicability and strong advantages in handling complex industrial applications.

4.1.3.3. Analysis of Dual-source Domain Results

To further validate the effectiveness of our proposed ESFBDA method, we conducted experiments under dual-source domain conditions. This involved learning from two source domains to predict the health status of the target domain. The experiment included six tasks, with detailed results presented in Table 9 and visualized in Fig. 13, Fig. 14, and Fig. 15.

1) Ablation Study Analysis

In the multi-source domain experiments, we first evaluated the contribution of each component in the ESFBDA method through an ablation study. The ablation setups included three groups: SFDA, SFBDA, and ESFDA, each representing the impact of different optimization steps on model performance.

The SFDA method, the most basic setup, combines SF with traditional MMD for domain alignment. As shown in Table 5, SFDA achieved an average classification accuracy of 74.80% with a standard deviation of 1.57. This indicates that when data comes from multiple source domains, the traditional SF and MMD combination struggles to capture common features across domains, leading to unstable classification performance.

Particularly when there are significant differences in data distribution between source domains, SFDA fails to effectively align features, resulting in greater variability.

Table 5. The accuracy comparison results of the method proposed in this paper and various other methods are presented herein (sourced from a dual domain).

Method	Average (%)	SD
SFDA	74.80	1.57
SFBDA	87.40	1.47
ESFDA	90.55	1.54
RSFDA	90.05	1.42
ASFDA	95.22	1.37
SFMCD	95.83	1.31
l_1/l_2-SFDA	94.25	1.56
ESFBDA	**99.15**	**0.83**

Building on SFDA, we introduced the Bootstrap optimization strategy to form the SFBDA method. Bootstrap enhances the robustness of MMD by resampling data, significantly improving the model's performance under multi-source domain conditions. Table 5 shows that SFBDA's average classification accuracy increased to 87.40%, with the standard deviation reduced to 1.47. Compared to SFDA, SFBDA performed more consistently across all six tasks (as shown in Fig. 13), indicating that Bootstrap optimization not only strengthens domain alignment robustness but also effectively reduces errors caused by differences in data distribution across source domains.
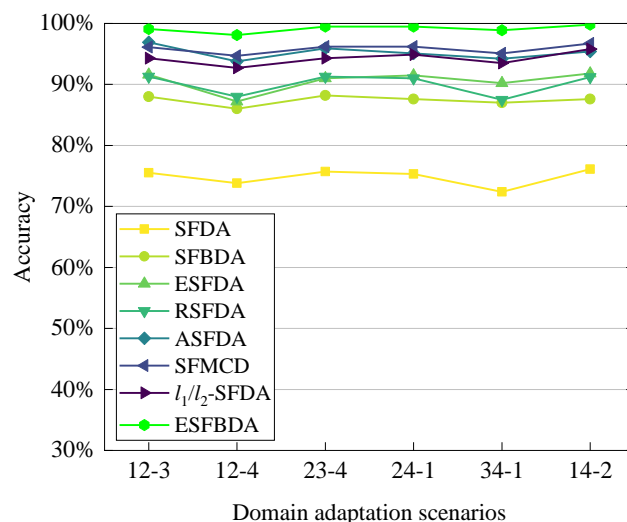
Fig. 13. Variable working conditions fault diagnosis outcomes of the proposed approach versus reference methodologies (sourced from a dual domain).
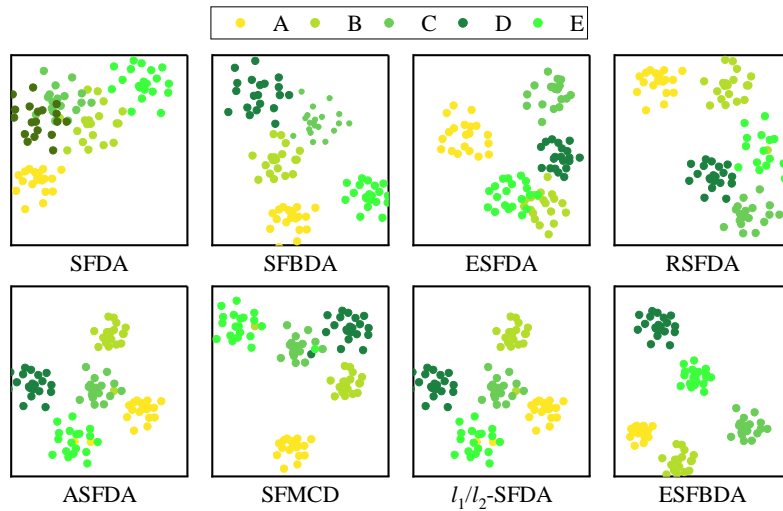
Fig. 14. Variable working conditions diagnostic results of various methods in the experiments for load 23-4 under small sample conditions.

Further enhancing SFBDA, we introduced ESF to create the ESFDA method. ESF optimizes the feature extraction process through row-column normalization and cosine similarity penalties, reducing feature redundancy and improving feature separation. Table 5 shows that ESFDA's average classification accuracy further increased to 90.55%, with the standard deviation reduced to 1.54. The performance curves in Fig. 13 and the clustering diagram in Fig. 14 demonstrate that the ESFDA method better captures common features under multi-source domain conditions and aligns cross-domain features, significantly improving classification accuracy. Notably, the ESF technique not only optimizes the structure of the feature space but also enhances the model's ability to distinguish between different fault types.

Through the ablation study comparison, it is clear that each component introduced significantly improves model performance. The basic SFDA method showed high variability due to its inability to effectively align multi-source domain data. The SFBDA method, with Bootstrap optimization, significantly enhanced the model's stability and accuracy across different source domains. The ESFDA method, with its optimized feature extraction and domain alignment process, further improved classification accuracy and model robustness, proving the critical role of each component in enhancing model performance.

Fig. 15 shows the confusion matrix results for different methods across six tasks. Compared to SFBDA, ESFDA significantly reduced classification errors across all tasks, demonstrating its superior performance under complex working conditions. Particularly in the integration of multi-source data, ESFDA effectively prevented the loss of feature information, ensuring highly accurate classification results.
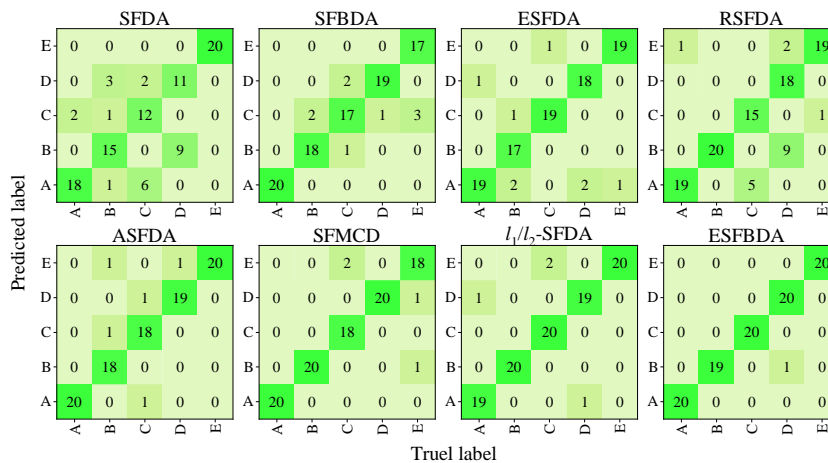
Fig. 15. Confusion matrix illustration of various methods in load 23-4 experiment.

2) Comparison with Existing Methods

After the ablation study, we compared the ESFBDA method with several advanced dual-source domain fault diagnosis methods. The data in Table 5, along with Fig. 13 through Fig. 15, strongly support this comparison.

As shown in Table 5, the ESFBDA method achieved an average classification accuracy of 99.15% with a standard deviation of only 0.83, demonstrating exceptional stability and outstanding classification accuracy. In comparison, the RSFDA method, which incorporates soft reconstruction penalties to improve feature representation, achieved an average classification accuracy of 90.05% with a standard deviation of 1.42. This suggests that while RSFDA can enhance feature diversity to some extent, excessive reconstruction may lead to the loss of critical fault features, particularly when handling multi-source data, where feature reconstruction consistency affects model generalization.

The ASFDA method measures domain differences using A-distance combined with sparse filtering for feature extraction. This method showed good classification ability under dual-source domain conditions, achieving an average classification accuracy of 95.22%, but still fell short of ESFBDA. This is mainly because ASFDA relies heavily on a single feature selection strategy based on A-distance, which makes it difficult to comprehensively capture common features across domains under multi-source conditions, thereby affecting overall model performance. In contrast, ESFBDA ensures comprehensive feature extraction and precise domain alignment by integrating Bootstrap optimization with Enhanced Sparse Filtering, leading to superior performance across different tasks.

The l_1/l_2-SFDA method, which enhances feature selection directionality by introducing l_1/l_2 norms, achieved an average classification accuracy of 94.25%, but with a standard deviation of 1.56, indicating some uncertainty in handling multi-source data. This uncertainty mainly stems from the l_1/l_2 norms overemphasizing certain features during selection, leading to feature loss or imbalance. ESFBDA, by integrating multiple optimization techniques, balances feature extraction comprehensiveness and accuracy, maintaining the highest classification accuracy and lowest variability in multi-source domain experiments.

The performance curves in Fig. 13 further illustrate the ESFBDA method's stable performance across tasks, consistently achieving the highest classification accuracy in almost all tasks, while other methods show varying degrees of fluctuation. The ESFBDA method's outstanding performance, particularly under complex multi-source working conditions, highlights its exceptional stability and robustness in industrial applications. The clustering diagram and confusion matrix in Fig. 14 and Fig. 15 further demonstrate the ESFBDA method's significant advantages in feature extraction and classification accuracy, with almost no misclassifications. These results not only validate the effectiveness of the ESFBDA method but also further solidify its leading position among existing methods.

Through the ablation analysis and comparison with similar methods, we have thoroughly validated the superior performance of the ESFBDA method in cross-condition fault diagnosis. With dual innovations in feature extraction and domain alignment, this method not only significantly improves classification accuracy but also exhibits remarkable stability and adaptability. Whether in the detailed analysis of the ablation study or the comprehensive comparison with existing methods, the ESFBDA method consistently excels, further reinforcing its potential for industrial fault diagnosis applications. These results provide strong theoretical support and experimental evidence for promoting this method in real-world industrial scenarios.

4.1.3.4. Analysis of Diagnostic Results with Different Source Domain Sample Sizes

In practical engineering applications, labeled monitoring data is often scarce. Therefore, fault diagnosis models for variable working conditions scenarios need to maintain high diagnostic accuracy even with limited samples. To assess the diagnostic performance of our proposed method under small-sample conditions for unknown conditions, the load 2-3 experiment was selected, and our proposed method, along with six comparative methods, was trained using varying percentages of training samples. Each result is the average of 20 random experiments, and the final diagnostic results are shown in Fig. 16. The training sample ratio represents the percentage of each class's training samples, for example, a 90% training sample ratio means that each class has 90% of the total training samples.

The results demonstrate that as the number of training

samples decreases, the diagnostic accuracy of all methods for variable working conditions scenarios decreases to some extent. Our proposed ESFBDA method consistently exhibits the highest diagnostic accuracy under small-sample conditions. As the number of training samples decreases, ESFBDA shows the smallest decline in diagnostic accuracy. Even with only 50% of the training samples, it still achieves a diagnostic accuracy of 94.9% with a standard deviation of 0.67%. The experiment shows that our method excels in small-sample variable working conditions fault diagnosis.
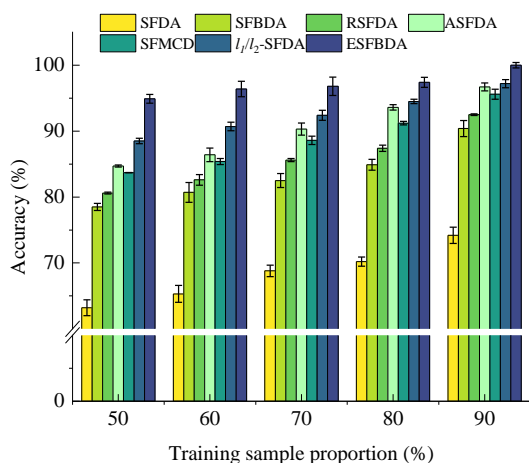
Fig. 16. Variable working conditions diagnostic results of various methods in the experiments for Load 2-3 under small sample conditions.

4.2. Case 2: bearing fault diagnosis

4.2.1. Data Preparation
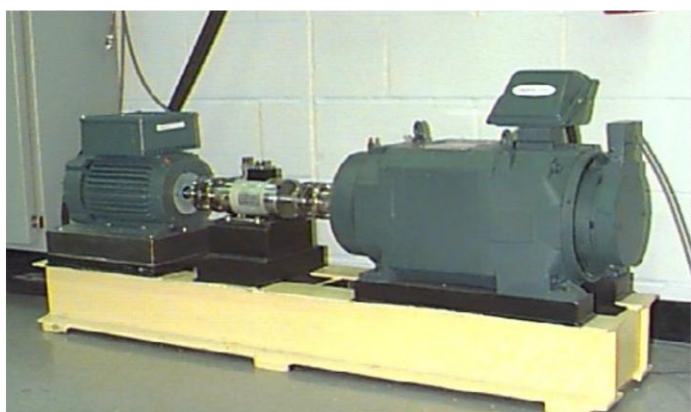
Fig. 18. Case western reserve university bearing data source [21].

To further validate the effectiveness of the ESFBDA method in addressing fault diagnosis under Variable Working Conditions, we utilized a dataset derived from bearing tests, as depicted in Figure 18, featuring the drive end bearing SKF6205-

2R [4]. The bearings were artificially damaged on the inner race, ball, and outer race through electrical discharge machining. Vibration signals were collected at a sampling rate of 12 kHz and a rotational speed of 1797 rpm under load conditions of 0, 1, 2, and 3 HP.

The detailed data selected, as outlined in Table 6, considers four health states: (1) Normal Health (NH); (2) Outer Race Fault (OF); (3) Inner Race Fault (IF); and (4) Ball Fault (BF), with a damage diameter of 7 mils.

Table 6. The description of bearing data.

Load (HP)	Fault size (mil)	Fault location
0		
1		
2	7	NH, IF, BF, OF
3		

4.2.2. Effectiveness Analysis

After completing experiment 1, we conducted ablation experiments and detailed comparisons with existing methods to further validate and support the performance of our proposed ESFBDA method under different working conditions. These experiments not only helped us understand the specific contribution of each method component to overall performance but also provided stronger evidence for the superiority of the ESFBDA method.

1) Ablation Study Analysis

Following the research approach in Section 4.1, we first conducted an in-depth analysis of the performance contributions of each component through ablation experiments. Table 7 and Fig. 17 show the fault diagnosis performance and accuracy metrics of different methods across various tasks.

As seen in Table 7, the classification accuracy significantly improved as we gradually enhanced the method's components. The SFDA method had an average classification accuracy of 82.24% with a standard deviation of 2.35, indicating high variability in performance under complex working conditions. By introducing the Bootstrap optimization strategy, the SFBDA method's average classification accuracy increased to 86.74%, and the standard deviation dropped to 1.29. This result validates the positive impact of Bootstrap on optimizing MMD calculations. However, it was only with the introduction of Enhanced Sparse Filtering in the ESFDA method that the classification accuracy further improved to 92.25%, with the

standard deviation significantly reduced to 1.00. This confirms the critical role of improved feature extraction techniques in cross-condition fault diagnosis.

Table 7. The accuracy comparison results of the method proposed in this paper and various other methods are presented herein.

Method	Average	SD
SFDA	82.24	2.35
SFBDA	86.74	1.29
ESFDA	92.25	1.00
RSFDA	94.48	1.27
ASFDA	96.20	0.65
SFMCD	97.05	0.73
l_1/l_2-SFDA	98.49	0.59
ESFBDA	99.52	0.27

Fig. 17 visually illustrates the performance changes of these methods across different tasks. It is evident that the ESFDA method consistently maintained high classification accuracy in all tasks, while the traditional SFDA and SFBDA methods showed greater variability. Fig. 18 further demonstrates the clustering effects of different methods in the feature space. The

feature points of the ESFBDA method are more concentrated, with clearer separation between classes, showcasing its strong capability in feature extraction.
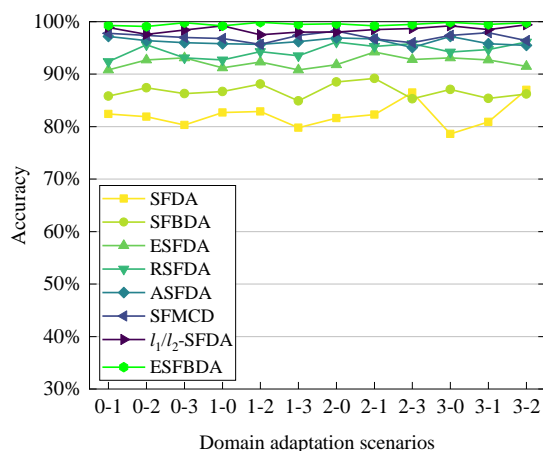
Fig. 17. Variable working conditions fault diagnosis outcomes of the proposed approach versus reference methodologies.
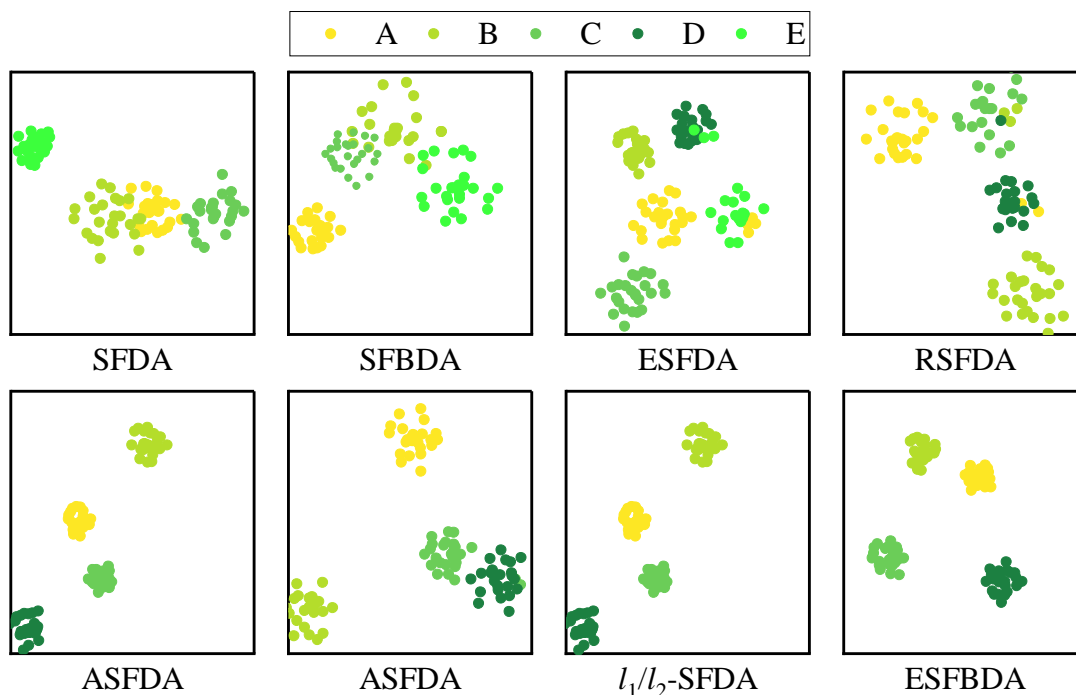
Fig. 18. Variable working conditions diagnostic results of various methods in the experiments for Load 3-1 under small sample conditions.

Fig. 19 shows the confusion matrices for each method across different tasks. The ESFBDA method achieved nearly 100% classification accuracy in all tasks, consistent with the accuracy data in Table 7, further proving its superiority and stability in

handling complex conditions. In contrast, the confusion matrices for the SFDA and SFBDA methods show more classification errors, indicating their limitations in dealing with complex working condition changes.
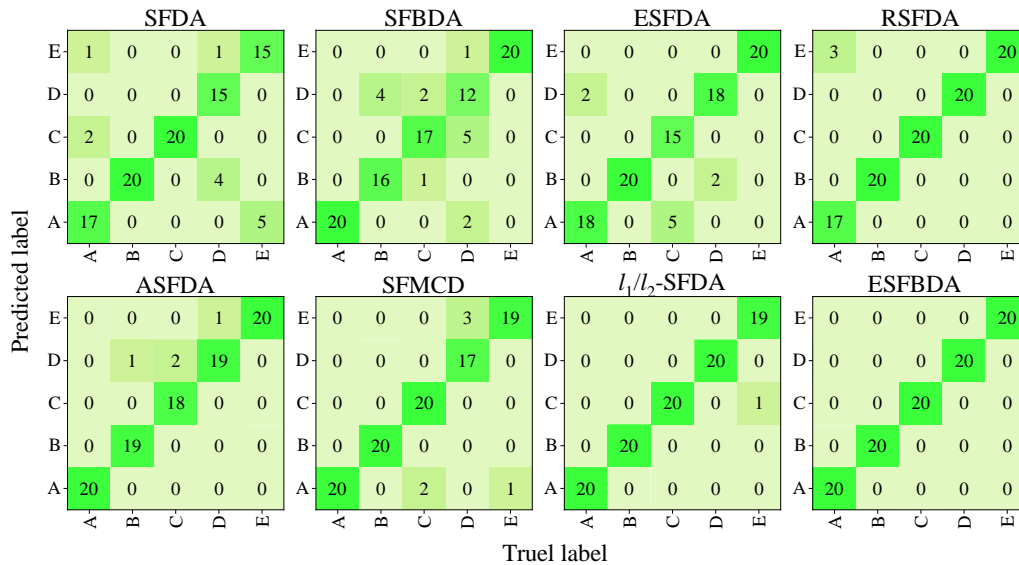
Fig. 19. Confusion matrix illustration of various methods in load 3-1 experiment.

2) Comparison with Existing Methods

To comprehensively validate the superiority of the ESFBDA method, we compared it with several advanced cross-condition fault diagnosis methods. The data in Table 7, along with the visualizations in Fig. 17 through Fig. 19, provide strong support for this comparison.

As shown in Table 7, the ESFBDA method achieved an average classification accuracy of 99.52%, with a standard deviation of only 0.27, demonstrating excellent stability and accuracy. For example, although the RSFDA method incorporated soft reconstruction penalties to improve feature extraction, its average classification accuracy was 94.48%, with a standard deviation of 1.27, indicating some variability under complex conditions. The ASFDA and l_1/l_2-SFDA methods achieved classification accuracies of 96.20% and 98.49%, respectively, but their stability and robustness still fell short compared to the ESFBDA method.

The curves in Fig. 17 further illustrate the stable performance of the ESFBDA method across all tasks, consistently achieving the highest classification accuracy. In contrast, the performance curves of other methods show greater variability, particularly under complex conditions where the ESFBDA method stands out. Fig. 18 and Fig. 19 further visually demonstrate the ESFBDA method's clear advantages in feature extraction and classification accuracy, with almost no misclassifications, fully confirming the method's effectiveness.

These subsequent experiments not only further validated the superior performance of the ESFBDA method in cross-condition fault diagnosis but also demonstrated how its dual innovations in feature extraction and domain alignment contribute to its significant advantages. Whether in the detailed analysis of the ablation study or the comprehensive comparison with existing methods, the ESFBDA method consistently exhibited high stability and accuracy, further reinforcing its potential for industrial fault diagnosis applications. These results provide strong theoretical support and experimental evidence for promoting this method in real-world industrial scenarios.

5. Conclusions

This paper introduces a variable working condition fault diagnosis method named ESFBDA, offering higher accuracy in cross-working condition fault diagnosis compared to existing SF-based domain adaptation methods. ESFBDA enhances SF technology by incorporating l_2 normalization and similarity penalty items, reducing feature loss. Additionally, it optimizes MMD using Bootstrap Resampling for more accurate domain difference assessment. Extensive experiments on a WT-Planetary Gearbox Fault dataset demonstrate its ability to accurately extract similar features across different working conditions and assess domain differences effectively, thus improving variable working condition fault diagnosis. Specifically, the application of our ESFBDA method to the WT-Planetary Gearbox dataset underscores its significant impact on enhancing fault diagnosis for wind turbine systems. This approach not only showcases the method's effectiveness in

a real-world context but also illuminates its potential to advance fault diagnosis techniques, ensuring the reliability and safety of such critical systems in the industry.

As for future avenues of exploration, there is potential in amalgamating conditional MMD or multi-kernel MMD with the ESFBDA model. Such integration might unlock further enhancements in the method's overall performance and robustness, solidifying its practical applications in pertinent areas. In addition, future work will critically examine the distinct impacts of column and row normalization in the ESFBDA method, aiming to refine SF for fault diagnosis. This exploration is essential for advancing DA techniques and optimizing performance in varying conditions.

References

1. Alquier P, Chérief-Abdellatif B-E, Derumigny A, Fermanian J-D. Estimation of copulas via maximum mean discrepancy. Journal of the American Statistical Association. 2023;118(543):1997-2012. https://doi.org/10.1080/01621459.2021.2024836

2. An Y, Zhang K, Chai Y, Liu Q, Huang X. Domain adaptation network base on contrastive learning for bearings fault diagnosis under variable working conditions. Expert Systems with Applications. 2023;212:118802. https://doi.org/10.1016/j.eswa.2022.118802

3. Bao H, Yan Z, Ji S, Wang J, Jia S, Zhang G, et al. An enhanced sparse filtering method for transfer fault diagnosis using maximum classifier discrepancy. Measurement Science and Technology. 2021;32(8):085105. https://doi.org/10.1088/1361-6501/abe56f

4. Center BD. Case western reserve university bearing data [Internet]. Cleveland, Ohio, U.S. Case School of Engineering. Available from: http://csegroups, case. ed./bearingdatacenter/pages/down-loaddata-file

5. Chopra P, Yadav SK. Restricted Boltzmann machine and softmax regression for fault detection and classification. Complex & Intelligent Systems. 2018;4:67-77. https://doi.org/10.1007/s40747-017-0054-8

6. Ding Y, Jia M, Zhuang J, Cao Y, Zhao X, Lee C-G. Deep imbalanced domain adaptation for transfer learning fault diagnosis of bearings under multiple working conditions. Reliability Engineering & System Safety. 2023;230:108890. https://doi.org/10.1016/j.ress.2022.108890

7. Gao T, Yang J, Tang Q. A multi-source domain information fusion network for rotating machinery fault diagnosis under variable operating conditions. Information Fusion. 2024;106:102278. https://doi.org/10.1016/j.inffus.2024.102278

8. Gould NI, Porcelli M, Toint PL. Updating the regularization parameter in the adaptive cubic regularization algorithm. Computational optimization and applications. 2012;53:1-22. https://doi.org/10.1007/s10589-011-9446-7

9. Griffin D, Lim J. Signal estimation from modified short-time Fourier transform. IEEE Transactions on acoustics, speech, and signal processing. 1984;32(2):236-243. https://doi.org/10.1109/TASSP.1984.1164317

10. Han C, Lei Y, Xie Y, Zhou D, Gong M. Visual domain adaptation based on modified A− distance and sparse filtering. Pattern Recognition. 2020;104:107254. https://doi.org/10.1016/j.patcog.2020.107254

11. Ji S, Han B, Zhang Z, Wang J, Lu B, Yang J, et al. Parallel sparse filtering for intelligent fault diagnosis using acoustic signal processing. Neurocomputing. 2021;462:466-477. https://doi.org/10.1016/j.neucom.2021.08.049

12. Jiang M, Liang Y, Feng X, Fan X, Pei Z, Xue Y, et al. Text classification based on deep belief network and softmax regression. Neural Computing and Applications. 2018;29:61-70. https://doi.org/10.1007/s00521-016-2401-x

13. Li W, Huang R, Li J, Liao Y, Chen Z, He G, et al. A perspective survey on deep transfer learning for fault diagnosis in industrial scenarios: Theories, applications and challenges. Mechanical Systems and Signal Processing. 2022;167:108487. https://doi.org/10.1016/j.ymssp.2021.108487

14. Liu D, Cui L, Cheng W. A review on deep learning in planetary gearbox health state recognition: Methods, applications, and dataset publication. Measurement Science and Technology. 2023. https://doi.org/10.1088/1361-6501/acf390

15. Ma L, Yang P, Peng K. Multitask Learning Based Collaborative Modeling of Heterogeneous Data for Compound Fault Diagnosis in Manufacturing Processes. IEEE Transactions on Industrial Informatics. 2024. https://10.1109/TII.2024.3441652

16. Ma Y, Shan C, Gao J, Chen H. Multiple health indicators fusion-based health prognostic for lithium-ion battery using transfer learning and hybrid deep learning method. Reliability Engineering & System Safety. 2023;229:108818. https://doi.org/10.1016/j.ress.2022.108818

17. Pang B, Liu Q, Sun Z, Xu Z, Hao Z. Time-frequency supervised contrastive learning via pseudo-labeling: An unsupervised domain adaptation network for rolling bearing fault diagnosis under time-varying speeds. Advanced Engineering Informatics. 2024;59:102304.

https://doi.org/10.1016/j.aei.2023.102304

18. Qian Q, Wang Y, Zhang T, Qin Y. Maximum mean square discrepancy: a new discrepancy representation metric for mechanical fault transfer diagnosis. Knowledge-Based Systems. 2023;276:110748. https://doi.org/10.1016/j.knosys.2023.110748

19. Schwendemann S, Amjad Z, Sikora A. Bearing fault diagnosis with intermediate domain based layered maximum mean discrepancy: A new transfer learning approach. Engineering Applications of Artificial Intelligence. 2021;105:104415. https://doi.org/10.1016/j.engappai.2021.104415

20. Shi Y, Deng A, Ding X, Zhang S, Xu S, Li J. Multisource domain factorization network for cross-domain fault diagnosis of rotating machinery: An unsupervised multisource domain adaptation method. Mechanical Systems and Signal Processing. 2022;164:108219. https://doi.org/10.1016/j.ymssp.2021.108219

21. Smith WA, Randall RB. Rolling element bearing diagnostics using the Case Western Reserve University data: A benchmark study. Mechanical systems and signal processing. 2015;64:100-131. https://doi.org/10.1016/j.ymssp.2015.04.021

22. Wang C, Zhu G, Liu T, Xie Y, Zhang D. A sub-domain adaptive transfer learning base on residual network for bearing fault diagnosis. Journal of Vibration and Control. 2023;29(1-2):105-117. https://doi.org/10.1177/10775463211042976

23. Wang H, Li C, Ding P, Li S, Li T, Liu C, et al. A Novel Transformer-based Few-Shot Learning Method for Intelligent Fault Diagnosis with Noisy Labels under Varying Working Conditions. Reliability Engineering & System Safety. 2024:110400. https://doi.org/10.1016/j.ress.2024.110400

24. Wang J, Ji S, Han B, Bao H. Intelligent fault diagnosis for rotating machinery using L1/2-SF under variable rotational speed. Proceedings of the Institution of Mechanical Engineers, Part D: Journal of Automobile Engineering. 2021;235(5):1409-1422. https://doi.org/10.1177/0954407020964625

25. Yao Y, Wang H. Optimal subsampling for softmax regression. Statistical Papers. 2019;60:585-599. https://doi.org/10.1007/s00362-018-01068-6

26. Yu X, Wang Y, Liang Z, Shao H, Yu K, Yu W. An adaptive domain adaptation method for rolling bearings' fault diagnosis fusing deep convolution and self-attention networks. IEEE Transactions on Instrumentation and Measurement. 2023;72:1-14. https://10.1109/TII.2024.3441652

27. Zennaro FM, Chen K. Towards understanding sparse filtering: A theoretical perspective. Neural Networks. 2018;98:154-177. https://doi.org/10.1016/j.neunet.2017.11.010

28. Zhang G, Han B, Li S, Wang J, Wang X. General normalized maximum mean discrepancy: intelligent fault identification method for bearings and gears under unstable conditions. Measurement Science and Technology. 2021;32(10):104001. https://doi.org/10.1088/1361-6501/abf3fb

29. Zhang Y, Han D, Tian J, Shi P. Domain adaptation meta-learning network with discard-supplement module for few-shot cross-domain rotating machinery fault diagnosis. Knowledge-Based Systems. 2023;268:110484. https://doi.org/10.1016/j.aei.2023.102304

30. Zhang Y, Ji J, Ma B. Reciprocating compressor fault diagnosis using an optimized convolutional deep belief network. Journal of Vibration and Control. 2020;26(17-18):1538-1548. https://doi.org/10.1177/1077546319900115

31. Zhang Z, Huang W, Liao Y, Song Z, Shi J, Jiang X, et al. Bearing fault diagnosis via generalized logarithm sparse regularization. Mechanical Systems and Signal Processing. 2022;167:108576. https://doi.org/10.1016/j.ymssp.2021.108576

32. Zhang Z, Yang Q. Unsupervised feature learning with reconstruction sparse filtering for intelligent fault diagnosis of rotating machinery. Applied Soft Computing. 2022;115:108207. https://doi.org/10.1016/j.asoc.2021.108207

33. Zhou Z. Fault diagnosis method for imbalanced and unlabeled data based on bayesian graph balanced learning. Measurement Science and Technology. 2024;35(9):096131. https://doi.org/10.1177/10775463241272933

34. Zhou Z, Chen W. Adaptive multi-scale graph fusion for fault diagnosis in concurrent variable conditions and unlabeled data. Journal of Vibration and Control. 2024:10775463241272933. https://doi.org/10.1088/1361-6501/ad5905

35. Zhou Z, Chen W, Yang C. Adaptive range selection for parameter optimization of VMD algorithm in rolling bearing fault diagnosis under strong background noise. Journal of Mechanical Science and Technology. 2023;37(11):5759-5773. https://doi.org/10.1007/s12206-023-1015-3